Nat. Hazards Earth Syst. Sci. Discuss., doi:10.5194/nhess-2016-1, 2016
Manuscript under review for journal Nat. Hazards Earth Syst. Sci.
Published: 23 February 2016

Natural Hazards and Earth System Sciences
Discussions

Multi-objective optimization of typhoon inundation forecast models for water-level gauging network by integration of ARMAX with a Genetic Algorithm

Huei-Tau Ouyang[1]

[1]Department of Civil Engineering, National Ilan University, Yilan City, 26047, Taiwan

Correspondence to: Huei-Tau Ouyang (htouyang@niu.edu.tw)

Abstract. The forecasting of inundation levels during typhoons requires that multiple objectives be taken into account, including the forecasting capacity with regard to variations in water level throughout the entire weather event, the accuracy that can be attained in forecasting peak water levels and the time at which peak water levels are likely to occur. This paper proposed a means of forecasting inundation levels in real-time using monitoring data from a water-level gauging network. ARMAX was used to construct water-level forecast models for each gauging station using input variables including cumulative rainfall and water level data from other gauging stations in the network. Analysis of the correlation between cumulative rainfall and water level data makes it possible to obtain an approximation as to the cumulative duration of rainfall and time lags associated with each gauging station. Analyses on water levels as well as on cumulative rainfall enable the identification of associate sites pertained to each gauging station that share high correlations with regard to water level and low mutual information with regard to cumulative rainfall. Water level data from associate sites is used as a second input variable for the water-level forecast model of the target site. Three indices were considered in the selection of an optimal model: the coefficient of efficiency (CE), error in the stage of peak water level (ESP), and relative time shift (RTS). We used a multi-objective genetic algorithm to derive an optimal Pareto set of models capable of performing well in the three objectives. A case study was conducted on the Xinnan area of Yilan County, Taiwan in which optimal water-level forecast models were established for each of the four water-level gauging stations in the area. Test results demonstrate that the model best able to satisfy PE exhibited significant time shift, whereas the models best able to satisfy CE and RTS provide accurate forecasts of inundations when variations in water level are less extreme.

Keyword: ARMAX, Multi-objective optimization, Genetic Algorithm, Water-level gauging network, Inundation, Typhoon

1 Introduction

Typhoons are common weather events in subtropical regions of the Pacific, between July and October. Heavy rains carried in by typhoons often lead to the severe inundation of low-lying areas, which can damage property and even threaten the safety of human lives. Limitations in funding for construction of flood control systems pose limits to the protective capacity

Nat. Hazards Earth Syst. Sci. Discuss., doi:10.5194/nhess-2016-1, 2016
Manuscript under review for journal Nat. Hazards Earth Syst. Sci.
Published: 23 February 2016

Natural Hazards and Earth System Sciences Discussions

of structural measures for disaster mitigation. When the scale of a typhoon exceeds construction design limits, non-structural means are required to prevent disasters associated with typhoons. The real-time forecasting of changes in inundation depth in the hours after a typhoon is a crucial factor in the planning of relief operations.

Considerable research has been conducted on inundation simulations and forecasting techniques, most of which can be roughly divided into two approaches: numerical simulations and black-box modellings. In numerical simulations, various physical phenomena that occur between rainfall and inundation are examined before carrying out theoretical derivations using mathematical analysis, after which solutions are obtained by numerical methods. This approach is based on a sound theoretical foundation and enables a clear representation of the physical mechanisms associated with inundation. The accuracy of the results makes them particularly useful in the forecasting of inundation in the absence of onsite observation data. However, this type of approach requires considerable computing resources and can be very time-consuming, which makes it difficult to provide forecast information in real-time for immediate disaster relief actions during typhoons. Black-box modellings are implemented in an entirely different manner. The process that occurs between rainfall and inundation is regarded as a black box, and no attempt is made to understand the underlying physical mechanisms. Rather, the relationships between inputs and outputs of the system are analyzed as a means of creating a black-box model. Although this approach is unable to explain the physical phenomena, however, it provides an accurate representation of the relationship between inputs and outputs. Calculations can generally be completed more rapidly (Karlsson and Yakowitz, 1987), and information related to future variations in water-level in inundated areas can be obtained in real-time, which can be immensely helpful to decision making and disaster prevention.

A number of studies have applied black-box models to the problems of inundation or flooding. Karunanithi et al. (1994) proposed a cascade-correlation algorithm for the selection of neural network architectures and a training algorithms and obtained encouraging results with regard to flow prediction. Thirumalaiah and Deo (1998) proposed the training of neural networks using a selected sequence of previous flood observations at a specific location to enable real-time flood forecasting. Toth et al. (2000) compared the advantages and limitations of Auto-Regressive Moving Average (ARMA), Artificial Neural Network (ANN), and the non-parametric nearest-neighbors method in rainfall-runoff forecasting. They concluded that time-series analysis is far more accurate than simple rainfall predictions of a heuristic nature. Change and Chen (2001) proposed a counter-propagation fuzzy-neural network (CFNN) capable of automatically generating rules for use in clustering input data to enable streamflow prediction. Nayak et al. (2005) employed fuzzy computation in the development of a real-time flood forecasting model. They concluded that the recursive use of a one-step-ahead forecast model to predict flow using longer lead times produces results better than those achieved using independent fuzzy models for the forecasting of flow under various lead times. Chen et al. (2005) constructed a flood forecast model using an adaptive neuro-fuzzy inference system (ANFIS). Their results demonstrated that ANFIS is superior to back-propagation neural network (BPNN). Romanowicz et al. (2008) developed a data-based mechanistic methodology ~~tfor~~ the derivation of nonlinear dependence between water levels measured at gauging stations along a river. Kia et al. (2011) developed a flood model using various flood causative factors using ANN techniques and geographic information system (GIS) for the modeling and simulation of flood-prone areas in the

Nat. Hazards Earth Syst. Sci. Discuss., doi:10.5194/nhess-2016-1, 2016
Manuscript under review for journal Nat. Hazards Earth Syst. Sci.
Published: 23 February 2016

Natural Hazards and Earth System Sciences Discussions

southern parts of Peninsular Malaysia. Pan et al. (2011) presented a real-time rainfall-inundation forecasting model using a hybrid neural network based on a synthetic database of inundation potential. Shiri et al. (2012) compared the performance of gene expression programming (GEP), adaptive neuro-fuzzy inference systems (ANFIS), and artificial neural networks (ANNs) in the forecasting of daily stream flow. They concluded that the GEP model outperformed the ANN and ANFIS models. Chen et al. (2012) utilized an ANN model and an ANFIS model to correct calculations in a two-dimensional hydrodynamic model used for the prediction of storm surge height during typhoon events. Najafzadeh and Zahii (2015) proposed the use of a neuro-fuzzy-based group method of data handling (NF-GMDH) as an adaptive learning network for the prediction of flow discharge in straight compound channels.

In this study, we sought to develop a method for the forecasting of inundation levels, based on data from a water-level gauging network during typhoons. We also performed a case study in which crucial model input variables were obtained by analyzing records from previous typhoons. Autoregressive moving average with exogenous inputs (ARMAX) was used to construct rainfall and water-level relationship models of the gauging stations, and three indices were defined for the evaluation of model performance. A Pareto optimal model set was identified for the three indices using a multi-objective genetic algorithm. Predicted water levels were compared with measured data to exam the performance of the optimal models subjected to each index.

This paper is organized as follows. The environmental background of the study area is introduced in Section 2. In Section 3, we explain ARMAX and the data analysis methods used to find suitable model input variables. We also introduce the indices used for the evaluation of the models. Section 4 presents the method used to identify the Pareto optimal model set for the evaluation indices using a multi-objective genetic algorithm. Section 5 discusses the forecasting capability of the optimal models for each objective based on search results. Conclusions follow in Section 6.

2 Study area

Yilan County (Fig. 1) is situated in the northeastern part of Taiwan. It has a sub-tropical monsoon climate and is famed for its rainy weather. With over 200 rain days per year, the annual average precipitation ranges between 2000 and 2500 mm. Yilan is bordered by mountains to the west and the ocean to the east. Typhoons are common in summer and autumn. Statistically, an average of two to three typhoons hit Taiwan each year, 45% of which make landfall in Yilan County (Pan et al., 2014). Severe inundations quickly form in low-lying areas during typhoons. Among the inundation-prone regions, the area of Xinnan is one of the worst.

The Xinnan area (Fig. 1) is located near the mouths of two major waterways in the county: the Meifu drainage waterway to the north and the Lanyang River to the south. Flat terrain dips to the east, and its eastern border abuts the Pacific. The average elevation in the area is just about 2 m above sea level. During typhoons, water levels in the two major waterways rise swiftly from large inflows upriver. The levees of the two waterways prevent runoff in the area from being drained out

Nat. Hazards Earth Syst. Sci. Discuss., doi:10.5194/nhess-2016-1, 2016
Manuscript under review for journal Nat. Hazards Earth Syst. Sci.
Published: 23 February 2016

Natural Hazards and Earth System Sciences Discussions

effectively, which soon leads to severe inundation. The safety and property of residents are in risk during typhoons, which underlines the need for effective disaster prevention measures.

In an attempt to better understand local inundation conditions during typhoons, the Water Resources Agency established the Surveillance Network for Typhoon Inundation in the Xinnan Area (SNTIX) in 2011. The Network includes four gauging stations receiving water-level data on-site the area, and a data transmission system receiving precipitation observation data from the QPESUMS (Quantitative Precipitation Estimation and Segregation using Multiple Sensor, Gourley et al., 2002) of the Central Weather Bureau. Table 1 lists detailed information related to the gauging stations, the locations of which are marked in Fig. 1. SNTIX reports local inundation levels via radio transmission every 10 minutes during typhoons, while QPESUMS transmits ten-minute rainfall in the area via internet connection at the same frequency. Figure 2 presents the water levels recorded by SNTIX at gauging stations and the QPESUMS rainfall data during Typhoon Trami in 2013. QPESUMS was developed jointly by the Central Weather Bureau and the National Severe Storm Laboratory (NSSL) in 2002, with a view to improving the accuracy of quantitative rainfall forecasts. QPESUMS comprises eight Doppler radar stations, each of which scans a radius of approximately 230 km. The system divides Taiwan into 441×56 grids, each covering 1.25×1.25 km2. Rainfall estimation is achieved by obtaining readings from 406 rainfall gauges and 45 ground stations for adjustments. QPESUMS forecasts future rainfall patterns by predicting the movement paths of cloud cells. Data is provided for a wide range of applications, including typhoon rainfall forecasts (Lee et al., 2006), river flooding forecasts (Vieux et al., 2003), and landslide forecasts (Chen et al., 2004).

Since its implementation, SNTIX has recorded data from ten typhoon events, as shown in Table 2. In addition to providing rainfall and water level information at the time of the typhoon, these records can also be used to develop water-level forecast models for gauging stations.

3 Model construction

To plant effective disaster prevention and relief operations during typhoons, it is crucial that one has the capacity to forecast inundation levels developing in the following hours. In the Xinnan area, inundation develops swiftly during typhoons, so forecasting must be quick and effective in order to provide sufficient lead time for decision making and operational planning. Thus, we adopted the ARMAX black-box model for the construction of water-level forecast models for gauging stations. It should be noted that during typhoons, response plans rely more heavily on water-levels than on runoff. We therefore based the forecast model on this study in the relationship between rainfall and water level rather than on the relationship between rainfall and runoff, as was common in many studies. Moreover, the rainfall and water level data in this study was not processed in the conventional manner, in which the data is normalized by the maximum and minimum values before performing model regression, considering the fact that these information cannot be obtained while a typhoon is in progress. To enable real-time water-level forecasting during typhoons, we designed the water-level forecast model using raw rainfall and water level data as inputs with the forecast water level of the next time step as the output.

Nat. Hazards Earth Syst. Sci. Discuss., doi:10.5194/nhess-2016-1, 2016
Manuscript under review for journal Nat. Hazards Earth Syst. Sci.
Published: 23 February 2016

3.1 ARMAX model

ARMAX (Box and Jenkins, 1976) is a linear black-box model that merges the AR model (Yule, 1927) and MA model (Slutsky, 1937) for time series analysis. It takes into account the influence of other external variables in the forecasting of future changes in dynamic systems. The model is as follows:

$$A(q)y(t) = \sum_{i=1}^{nu} B_i(q)u_i(t - nk_i) + C(q)e(t)\ , \quad (1)$$

where y denotes the output of the system, u_i stands for the exogenous input for input i, nu indicates the number of inputs, nk_i is the time lag for each input, e is the error term, and $A(q)$, $B_i(q)$, and $C(q)$ are the polynomial functions composed of time-shift operator q.

In this study, y represents the water levels recorded at the gauging stations. To make full use of monitoring data from the surveillance network, each water level model contains two exogenous inputs: rainfall data u_1 from QPESUMS and water level data u_2 from an associate gauging station. The structure of the model is determined by the number of terms in the four polynomial functions $A(q)$, $B_1(q)$, $B_2(q)$, and $C(q)$ and the time lags of the two exogenous inputs, nk_1 and nk_2. The coefficients of four polynomial functions $A(q)$, $B_1(q)$, $B_2(q)$, and $C(q)$ can be obtained by calibrating rainfall and water level data.

3.2 Determination of input variables

In this study, we set the cumulative rainfall as the first input variable. After calculating the cumulative rainfall of various durations from 1 hour to 30 hours, the results are subjected to correlation analysis using water level data from the target site to derive the correlation coefficient (CC), which is defined as

$$\mathrm{CC(x,y)} = \frac{cov(x,y)}{\sigma_x \sigma_y} = \frac{\sum_{i=1}^{n}(x_i-\bar{x})(y_i-\bar{y})}{\sqrt{\sum_{i=1}^{n}(x_i-\bar{x})^2}\sqrt{\sum_{i=1}^{n}(y_i-\bar{y})^2}}\ , \quad (2)$$

where cov refers to the covariance between variables x and y; σ_x and σ_y are the standard deviations of x and y, respectively, and n denotes the number of data points. CC ranges from -1 to 1, which respectively indicate perfect negative correlation and perfect positive correlation between x and y, while a CC value of 0 indicates the complete absence of correlation.

Figures 3(a) through 3(d) present the results of correlation analysis pertaining to water-level data from various gauging stations and cumulative rainfall of various durations. The black round dots in the figures mark the average CC values of each typhoon event, and the tops and bottoms of the bars indicate the maximum and minimum CC values among the events. The variations in the average CC in the figures clearly show that the average CC increases with the duration of cumulative rainfall, reaches a peak, and then declines gradually. This phenomenon is apparent in all of the gauging stations. However, the duration of cumulative rainfall corresponding to the peak average CC can vary. Table 3 lists the peak average CC, the corresponding duration of cumulative rainfall, and the maximum and minimum CCs measured at each station. As can be seen, the peak average fluctuates roughly between 0.7 and 0.9, which indicates that a certain degree of correlation exists

Nat. Hazards Earth Syst. Sci. Discuss., doi:10.5194/nhess-2016-1, 2016
Manuscript under review for journal Nat. Hazards Earth Syst. Sci.
Published: 23 February 2016

Natural Hazards and Earth System Sciences Discussions

between water level and cumulative rainfall at the stations. The table also shows that the duration of cumulative rainfall corresponding to the peak average CC is longer in stations located further downward in the area. For instance, the duration of cumulative rainfall corresponding to the peak average CC at the Zonnanxin station, which is at higher ground in the area, is 18 hr, whereas the duration at the Meifu station, which is closest to the sea, is 25 hr. We speculate that this might be associated with the time needed for water to aggregate and move downward. The table also presents a slight decrease in the peak average CC as the station falls ~~closers~~ to the sea as well as a greater difference between the maximum and minimum CC values. It is possible that this is because water levels at locations closer to the sea are influenced by ocean tides, which somewhat reduces its correlation with cumulative rainfall.

After identifying the duration of cumulative rainfall with the highest correlation for each gauging station, we analyzed the time lags between water levels and cumulative rainfall. We shifted back the cumulative rainfall data one time step at a time (each time step is 10 minutes) and calculated the CCs between water level and cumulative rainfall for each station. Figures 4(a) through 4(d) display the results of cross-correlation analysis for water levels and cumulative rainfall at each station. As can be seen, the peak average CC for each station occurred at zero lag, and the average CC decreases as the leg lengthened. This indicates that no time lag exists between water level and cumulative rainfall. Furthermore, the figures show that as the lag increased, not only the average but also the maximum and minimum CCs decreased, and the difference between the maximum and minimum CCs (ΔCC) gradually increased. This demonstrates that for all events the correlation between water level and cumulative rainfall during typhoons diminishes with the length of the lag.

To make full use of the water level records from the gauging stations, we identified an associate station for each existing station and used the water levels from the associate station as a second input variable of the forecast models. Generally speaking, the input and output of a model require a higher degree of correlation, while in between the input variables a lower mutual information (MI) is expected (Bowden et al., 2005; Talei et al., 2010; Maier et al., 2010) in order to ensure that the information provided to the model from the inputs are not redundant. MI is defined as

$$\mathrm{MI}(x,y) = \frac{1}{2}\log\left(\frac{|C_{xx}||C_{yy}|}{C}\right), \tag{3}$$

where C is the covariance matrix defined as

$$\mathrm{C} = \begin{bmatrix} C_{xx} & C_{xy} \\ C_{yx} & C_{yy} \end{bmatrix}, \tag{4}$$

where C_{xx} and C_{yy} are the variance of variables x and y, respectively; C_{xy} and C_{yx} are the covariance of variables x and y; and $|C|$ is the determinant of the covariance matrix. An MI value equal to 0 indicates complete independence between x and y, while a higher MI value indicates stronger dependence between x and y (Fraser and Swinney, 1986; Moon et al., 1995).

To find an associate site with which the water-level data has a high CC with that of the target site while having a low MI with the identified cumulative rainfall of that specific site, we combined the two indices into

$$\mathrm{R} = \mathrm{CC} + (1 - \mathrm{MI}), \tag{5}$$

Nat. Hazards Earth Syst. Sci. Discuss., doi:10.5194/nhess-2016-1, 2016
Manuscript under review for journal Nat. Hazards Earth Syst. Sci.
Published: 23 February 2016

Natural Hazards and Earth System Sciences Discussions

The MI value presents the degree of dependence between the input variables; i.e., 1-MI reflects the degree of independence between input variables. The candidate site with the highest R value was designated as the associate site for a given target site. This approach in which MI is taken into account in the selection of model inputs has been employed in previous studies (Talei et al., 2010; Elshorbagy et al., 2010; He et al., 2011).

Table 4 lists the event-averaged CCs between water level data from each target site and their candidate sites, as well as the event-averaged MI of the first input variable (i.e., identified cumulative rainfall) of the target site and the water level data from the candidate sites. The table also presents the R values for each pair of sites. The asterisk notes the highest R values for each site, and the corresponding candidate sites were those selected as associate sites. The associate sites that were eventually selected for each target site are displayed at the bottom of Table 4.

To elucidate the meaning of the time lag prior to variations in water level data from target sites and their associate sites, we followed the previous analysis method in shifting water level data from the associate sites one time step at a time. We then calculated the CCs between the water level data from the target site and the associate site until we reached 30 time steps. The results in Fig. 5 show that the event-averaged CCs are all highest at zero lag. As the lag increases, the average, maximum, and minimum CCs of each station decrease, and the difference between the maximum and minimum CCs gradually increases. This is a clear indication that no time lag exists between variations in water level measured at target sites and at their associate sites.

The above data analysis makes it possible to determine the input variables of the water level models for each station as well as their time lags, as shown in Table 5. The first input variable is cumulative rainfall, and the duration of cumulative rainfall in the various stations are not the same; however, all of the time lags are 0. The second input variable is water level data from the associate site for which the time lags are also 0.

3.3 Model evaluation

The performance of each model was evaluated using the three indices below.

(1) Nash-Sutcliffe Coefficient of Efficiency (CE)

The Nash-Sutcliffe Coefficient of Efficiency was proposed by Nash and Sutcliffe (1970) to assess the forecasting capacity of hydrological models. It is defined as

$$\mathrm{CE} = 1 - \frac{\sum_{t=1}^{n}[y_{obs}(t) - y_{est}(t)]^2}{\sum_{t=1}^{n}[y_{obs}(t) - \bar{y}_{obs}]^2}, \quad (6)$$

where y_{obs} and y_{est} denote the observed and estimated water levels; $\bar{y}_{obs}$ is the average observed water level, and n indicates the number of data items. The CE value represents the goodness of fit between the observed data and the forecast results of the model; a CE value closer to 1 means that the water-level forecasts more closely match the observation data.

(2) Error in the stage of peak water-level (ESP)

Nat. Hazards Earth Syst. Sci. Discuss., doi:10.5194/nhess-2016-1, 2016
Manuscript under review for journal Nat. Hazards Earth Syst. Sci.
Published: 23 February 2016

Natural Hazards and Earth System Sciences Discussions

$$\mathrm{ESP} = \frac{|y_{p,est} - y_{p,obs}|}{d_{p,obs}}, \quad (7)$$

In the formula above, $y_{p,obs}$ and $y_{p,est}$ denote the peak observed and estimated water levels, respectively, and $d_{p,obs}$ is the peak observed water depth. ESP represents the error between the peak observed water level and the forecast results of the model. A smaller ESP value means that the estimated peak water levels more closely match the observed values.

(3) Relative Time Shift (RTS)

Previous researches have shown that using historical data to forecast future changes often results in time shift errors between the forecast and measured hydrographs (Dawson and Wilby, 1999; Jain et al., 2004; de Vos and Rientjes, 2005). To evaluate the time shift error of forecast water levels, we shifted the forecast water level hydrograph back by 1 to 18 time steps and then calculated the CE values. The time step corresponding to the highest CE value is the time shift error (δ) of the water level model. This method was also adopted by de Vos and Rientjes (2005) and Talei et al. (2010). The relative time shift (RTS) of the models in this study was defined as

$$\mathrm{RTS} = \frac{\delta}{L_t}, \quad (8)$$

where δ denotes time shift error of the model, and L_t is the prediction lead time of the model. A smaller RTS refers to a smaller time shift error between the forecast and observed water levels.

3.4 Cross validation

We adopted cross validation (Geisser, 1993) for typhoon event validation and model calibration in this study. We selected single typhoon events for validation with the rest typhoon events for model calibration. In turn, all of the typhoon events were validated. The calculation of evaluation indices were based on the validation results of each typhoon. The mean values for all validated events produced the average performance of the models.

4 Multi-objective optimization problem

For the evaluation of model performance, we used three indices: CE (to assess the capacity of a model to simulate entire typhoon events), PE (to assess peak water levels), and RTS (to determine the time at which a peak water level occurs). These elements are crucial to disaster prevention operations during typhoons and must therefore be considered simultaneously. Unfortunately, it is difficult to weigh the importance of each element. Thus, we employed multi-objective optimization to search for models capable of performing well in all three indices.

4.1 Objective functions and Design variables

The design goals included a larger CE and smaller PE and RTS. Thus, we defined the objective function as follows:

Objective 1: minimize $(1 - \overline{CE})$, (9)

Nat. Hazards Earth Syst. Sci. Discuss., doi:10.5194/nhess-2016-1, 2016
Manuscript under review for journal Nat. Hazards Earth Syst. Sci.
Published: 23 February 2016

Natural Hazards and Earth System Sciences Discussions

Objective 2: minimize $\overline{PE}$, (10)

Objective 3: minimize $\overline{RTS}$, (11)

where $\overline{CE}$, $\overline{PE}$, and $\overline{RTS}$ denote the typhoon-event averages of the three indices.

As mentioned previously, the structure of the ARMAX model is determined by the polynomial functions $A(q)$, $B_1(q)$, $B_2(q)$, and $C(q)$ and the time lags of the two exogenous inputs, nk_1 and nk_2. The time lags, nk_1 and nk_2, can be derived from previous data analysis. The analysis of time lag between cumulative rainfall and water levels at the associate site shows that the time lags between the two inputs and the output of the model are both 0. QPESUMS is able to provide forecasts on rainfall in the following time step; therefore, we set nk_1 to 0 in order to incorporate the rainfall predictions provided by QPESUMS within the models. Because we have only real-time monitoring values (rather than forecast values), for the water level at associate sites, therefore, we set nk_2 to 1. Thus, the structure of the model is determined by the remaining number of terms in the polynomial functions $A(q)$, $B_1(q)$, $B_2(q)$, and $C(q)$. Thus, we set the design variables as the number of terms in the four polynomial functions, which are integers and limited the range of each design variable to between 1 and 10 in order to preserve the simplicity of the model.

4.2 Multi-objective Genetic Algorithm

A lack of continuous relationships between the structure of the model and the objective function makes it impossible to obtain the optimal value of this problem using a gradient-based method. Based on the characteristics of the problem, we employed a genetic algorithm (GA) as a tool for optimization, due to the fact that GAs do not require the Hessian matrix of the objective function to derive the optimal solution for each design variable. Furthermore, the fact that GAs can search for global optimums (Goldberg, 1989) makes this an extremely suitable approach to the identification of an ideal model.

GAs are based on Darwin's theory of natural selection. Since Holland (1973) developed a sound mathematical foundation based on this principle, GAs have been widely applied in a variety of fields to solve problems that could not otherwise be solved using conventional methods. In GAs, the individuals in a group are viewed as possible solutions to the problem under discussion. The individuals are rated according to their performance as they pertain to the objective functions and constraints. Superior performance increases the chance of passing on genes to the next generation. Through this process, the overall performance of the population gradually evolves and improves. After evolving for several generations, individuals with optimal genes (i.e., those that dominate the population), are adopted as the optimal solutions to the problem. GAs conduct optimization by assessing the performance of individuals in the population, which makes them ideally suited to solving problems with multiple objectives.

We employed the multi-objective genetic algorithm in Matlab to search for the Pareto optimal set of the integer multi-objective optimization problem. The optimal model set contains models that perform well in all three indices. We set the population size at 50 and the Pareto fraction at 0.35. The maximum number of evolutionary generations was 200, and the GA was set to terminate after the results stalled for more than 20 generations.

Nat. Hazards Earth Syst. Sci. Discuss., doi:10.5194/nhess-2016-1, 2016
Manuscript under review for journal Nat. Hazards Earth Syst. Sci.
Published: 23 February 2016

Natural Hazards and Earth System Sciences Discussions

5 Result and discussion

The result of the multi-objective genetic algorithm is a Pareto optimal set. All of the models in this set are un-dominated, which means that at least one of their three indices (CE, PE, and RTS) is not surpassed by that of any other model. We selected the models with the best performance in all three indices from the Pareto optimal set, the results of which are as shown in Table 6. We listed three models for each gauging station and named them according to their location. For example the models for Zongnanxin station are Z1, Z2, and Z3. Among the three model types, Model Type 1 achieved the highest average CE, Model Type 2 achieved the lowest average PE, and Model Type 3 achieved the lowest average RTS. The table lists four integer design variables for each model, respectively indicating the number of terms in $A(q)$, $B_1(q)$, $B_2(q)$, and $C(q)$. The table also displays the scores of each model type on the three indices, wherein the score marked with an asterisk achieved the optimal value for that index.

Using data from Typhoon Saola, a water-level forecast was performed using the models of each gauging station with a lead time of 3 hr. We then compared the results with the observed values, as is shown in Figs. 6(a) through 6(d). The results in Fig. 6(a) show that the forecast water levels from the three models of the Zhongnanxin station (furthest from the sea), are roughly identical to the observed water levels, indicating that the forecast results are very accurate. No significant differences were observed among the forecast results of the three model types.

The forecast results of the other three gauging stations in Figs. 6(b), 6(c), and 6(d) by the three types of models present different characteristics. Model Type 2 (X2, S2, and M2) shows good performance in predicting peak water levels while exhibiting a time shift between the measured water levels and the water levels forecast. Model Type 2 emphasizes the need to minimize error in peak water levels; therefore, it is likely that variations in the water level forecasts from this model closely follow the changes in measured water levels with a certain degree of lag. In contrast, Model Type 1 (Z1, X1, S1, and M1) differs little from Type 3 (Z3, X3, S3, and M3) in Figs. 6(b), 6(c), and 6(d), both of which achieve perfect forecasts as water levels dropped but produce slight time lags as water level rose. This is particularly apparent at the Sijie station in Fig. 6(c) and at the Meifu station in Fig. 6(d), where water levels rose swiftly. However, the time shift errors presented by Model Types 1 and 3 are still smaller than 3 hr. Considering that the lead time used in these model forecasts was 3 hr, any time shift error of less than 3 hr means that the results retain reference value for disaster prevention operations during typhoons.

In the forecasting of peak water levels, the results in Figs. 6(b), 6(c), and 6(d) show Model Type 2 is superior over Model Types 1 and 3. On the other hand, in forecasting the time at which peak water levels are likely to occur, Model Types 1 and 3 are more accurate at all four stations. The ability to accurately determine the peak water levels as well as the arrival time of the peaks is extremely helpful for response operations during typhoons. All the three models provide valuable information and thus should all be considered in practice.

Nat. Hazards Earth Syst. Sci. Discuss., doi:10.5194/nhess-2016-1, 2016
Manuscript under review for journal Nat. Hazards Earth Syst. Sci.
Published: 23 February 2016

Natural Hazards and Earth System Sciences Discussions

6 Conclusion

This study developed a simple approach to the forecasting of variations in inundation levels during typhoons. The proposed method uses a network of water-level gauging station in conjunction with rainfall forecast data. ARMAX was used to construct water-level forecast models at each gauging site. Suitable input variables and lags in the water-level models were identified by analyzing historical data from typhoons in the past. A multi-objective genetic algorithm was used to derive a Pareto optimal set of models capable of performing well in three indices (CE, PE, and RTS) as well as to identify the water-level forecast model that obtained the best results at each gauging station. Comparisons with measured water levels shows that the model emphasizing PE resulted in accurate prediction on the peak water levels yet noticeable time lag. The models emphasizing CE and RTS provided an accurate indication of variations in water levels with no lag while water levels were dropping, yet a slight time lag when water levels were rising. The models emphasizing CE or RTS displayed good performance in forecasting the time at which peak water levels would occur, while the models emphasizing PE show good prediction on peak water levels. All three types of models provide information crucial to disaster prevention and relief operations in a timely manner during typhoons and thus should all be considered in practice.

Acknowledgements

This research was supported by the Ministry of Science and Technology in Taiwan under grant No. MOST 104-2625-M-197-001. Support from the Water Resources Agency in Taiwan is also gratefully acknowledged.

References

Bowden, G. J., Dandy, G. C., and Maier, H. R.: Input determination for neural network models in water resources applications. Part 1—background and methodology. Journal of Hydrology, 301(1), 75-92, 2005.

Box, G. E. and Jenkins, G. M.: Time series analysis: forecasting and control, revised ed, Holden-Day, 1976.

Chang, F. J. and Chen, Y. C.: A counterpropagation fuzzy-neural network modeling approach to real time streamflow prediction. Journal of hydrology, 245(1), 153-164, 2001.

Chen, C. Y., Lin, L. Y., Yu, F. C., Lee, C. S., Tseng, C. C., Wang, A. H., and Cheung, K. W: Improving debris flow monitoring in Taiwan by using high-resolution rainfall products from QPESUMS. Natural hazards, 40(2), 447-461,2007.

Chen, S. H., Lin, Y. H., Chang, L. C., and Chang, F. J.: The strategy of building a flood forecast model by neuro-fuzzy network. Hydrological Processes, 20(7), 1525-1540, 2006.

Chen, W. B., Liu, W. C., and Hsu, M. H.: Predicting typhoon-induced storm surge tide with a two-dimensional hydrodynamic model and artificial neural network model. Natural Hazards and Earth System Science, 12(12), 3799-3809, 2012.

Dawson, C. W., and Wilby, R.: An artificial neural network approach to rainfall-runoff modelling. Hydrological Sciences Journal, 43(1), 47-66, 1998.

de Vos, N. J., and Rientjes, T. H. M.: Constraints of artificial neural networks for rainfall-runoff modelling: trade-offs in hydrological state representation and model evaluation. Hydrology and Earth System Sciences Discussions Discussions, 2(1), 365-415, 2005.

Elshorbagy, A., Corzo, G., Srinivasulu, S., and Solomatine, D. P.: Experimental investigation of the predictive capabilities of data driven modeling techniques in hydrology-Part 1: Concepts and methodology. Hydrology and Earth System Sciences, 14(10), 1931-1941, 2010.

Fraser, A. M., and Swinney, H. L.: Independent coordinates for strange attractors from mutual information. Physical review A, 33(2), 1134, 1986.

Goldberg, D. E.: Genetic Algorithms in Search, Optimization, and Machine Learning. Addison Wesley, 1989.

Gourley, J. J., Maddox, R. A., Howard, K. W., and Burgess, D. W.: An exploratory multisensor technique for quantitative estimation of stratiform rainfall. Journal of Hydrometeorology, 3(2), 166-180, 2002.

He, J., Valeo, C., Chu, A., and Neumann, N. F.: Prediction of event-based stormwater runoff quantity and quality by ANNs developed using PMI-based input selection. Journal of hydrology, 400(1), 10-23, 2011.

Holland, J. H.: Genetic algorithms and the optimal allocation of trials.SIAM Journal on Computing, 2(2), 88-105, 1973.

Jain, A., Sudheer, K. P., and Srinivasulu, S.: Identification of physical processes inherent in artificial neural network rainfall runoff models.Hydrological Processes, 18(3), 571-581, 2004.

Karlsson, M. and Yakowitz, S.: Rainfall-runoff forecasting methods, old and new. Stochastic Hydrology and Hydraulics, 1(4), 303-318, 1987.

Karunanithi, N., Grenney, W. J., Whitley, D., and Bovee, K.: Neural networks for river flow prediction. Journal of Computing in Civil Engineering,8(2), 201-220, 1994.

Kia, M. B., Pirasteh, S., Pradhan, B., Mahmud, A. R., Sulaiman, W. N. A., and Moradi, A.: An artificial neural network model for flood simulation using GIS: Johor River Basin, Malaysia. Environmental Earth Sciences, 67(1), 251-264, 2012.

Lee, C. S., Huang, L. R., Shen, H. S., and Wang, S. T.: A climatology model for forecasting typhoon rainfall in Taiwan. Natural Hazards, 37(1-2), 87-105, 2006.

Maier, H. R., Jain, A., Dandy, G. C., and Sudheer, K. P.: Methods used for the development of neural networks for the prediction of water resource variables in river systems: current status and future directions. Environmental Modelling and Software, 25(8), 891-909, 2010.

Moddemeijer, R.: On Estimation of Entropy and Mutual Information of Continuous Distributions, Signal Processing, 16(3), 233-246, 1989.

Moon, Y. I., Rajagopalan, B., and Lall, U.: Estimation of mutual information using kernel density estimators. Physical Review E, 52(3), 2318-2321, 1995.

Najafzadeh, M. and Zahiri, A.: Neuro-Fuzzy GMDH-Based Evolutionary Algorithms to Predict Flow Discharge in Straight Compound Channels. Journal of Hydrologic Engineering, 20(12), 04015035, 2015.

Nash, J. and Sutcliffe, J. V.: River flow forecasting through conceptual models part I—A discussion of principles. Journal of hydrology, 10(3), 282-290, 1970.

Nayak, P. C., Sudheer, K. P., and Ramasastri, K. S.: Fuzzy computing based rainfall-runoff model for real time flood forecasting. Hydrological Processes, 19(4), 955-968, 2005.

Pan, T. Y., Chang, L. Y., Lai, J. S., Chang, H. K., Lee, C. S., and Tan, Y. C.: Coupling typhoon rainfall forecasting with overland-flow modeling for early warning of inundation. Natural Hazards, 70(3), 1763-1793, 2014.

Pan, T. Y., Lai, J. S., Chang, T. J., Chang, H. K., Chang, K. C., and Tan, Y. C.: Hybrid neural networks in rainfall-inundation forecasting based on a synthetic potential inundation database. Natural Hazards and Earth System Science, 11(3), 771-787, 2011.

Romanowicz, R. J., Young, P. C., Beven, K. J., and Pappenberger, F.: A data based mechanistic approach to nonlinear flood routing and adaptive flood level forecasting. Advances in Water Resources, 31(8), 1048-1056, 2008.

Geisser, S.: Predictive Inference, New York, NY: Chapman and Hall, 1993.

Shiri, J., Kişi, Ö., Makarynskyy, O., Shiri, A. A., and Nikoofar, B.: Forecasting daily stream flows using artificial intelligence approaches. ISH Journal of Hydraulic Engineering, 18(3), 204-214, 2012.

Slutzky, E.: The summation of random causes as the source of cyclic processes. Econometrica: Journal of the Econometric Society, 105-146, 1937.

Talei, A. and Chua, L. H.: Influence of lag time on event-based rainfall–runoff modeling using the data driven approach. Journal of Hydrology, 438, 223-233, 2012.

Talei, A., Chua, L. H. C., and Wong, T. S.: Evaluation of rainfall and discharge inputs used by Adaptive Network-based Fuzzy Inference Systems (ANFIS) in rainfall–runoff modeling. Journal of Hydrology, 391(3), 248-262, 2010.

Thirumalaiah, K., and Deo, M. C.: Real-time flood forecasting using neural networks. Computer-Aided Civil and Infrastructure Engineering, 13(2), 101-111, 1998.

Toth, E., Brath, A., and Montanari, A.: Comparison of short-term rainfall prediction models for real-time flood forecasting. Journal of Hydrology, 239(1), 132-147, 2000.

Vieux, B. E., Vieux, J. E., Chiarong, C., and Howard, K. W.: Operational deployment of a physics-based distributed rainfall-runoff model for flood forecasting in Taiwan. IAHS-AISH publication, 251-257, 2003.

Yule, G. U.: On a method of investigating periodicities in disturbed series, with special reference to Wolfer's sunspot numbers. Philosophical Transactions of the Royal Society of London. Series A, Containing Papers of a Mathematical or Physical Character, 267-298, 1927.

Nat. Hazards Earth Syst. Sci. Discuss., doi:10.5194/nhess-2016-1, 2016
Manuscript under review for journal Nat. Hazards Earth Syst. Sci.
Published: 23 February 2016

Natural Hazards and Earth System Sciences Discussions

Table 1 Water-level gauging network in Xinnan area

Gauging station	Location		Elevation above sea level (m)
	Longitude	Latitude	
Zhongnanxin	121.7877	24.7239	1.94
Xinnan	121.8012	24.7250	0.78
Sijie	121.8083	24.7234	0.13
Meifu	121.8156	24.7191	0.23

Table 2 Historical typhoon events recorded by SNTIX

Typhoon	Year	Time of official typhoon sea warning issued h/day/month (UTC)	Affecting period (hr)	Cumulative rainfall (mm)	Maximum rainfall intensity (mm/hr)
Songda	2011	0230/27/May	36	191.6	28.5
Nanmadol	2011	0530/27/Aug	99	159.6	26.5
Saola	2012	2030/30/Jul	90	506.1	35.5
Soulik	2013	0830/11/Jul	63	138.0	30.0
Trami	2013	1130/20/Aug	45	160.1	21.5
Usagi	2013	2330/19/Sep	63	158.2	24.0
Matmo	2014	1730/21/Jul	54	107.5	34.0
Fung-wong	2014	0830/19/Sep	72	79.5	37.5
Soudelor	2015	1130/6/Aug	69	462.5	86.0
Dujuan	2015	0830/27/Sep	57	226.0	41.5

Table 3 Correlation coefficient (CC) between water-level and cumulative rainfall with average peak and the associated duration of cumulative rainfall

Gauging site	CC between water-level and cumulative rainfall				Duration of cumulative rainfall (hr)
	Average peak	Maximum	Minimum	ΔCC	
Zongnanxin	0.910	0.952	0.856	0.096	18
Xinnan	0.822	0.956	0.651	0.305	20
Sijie	0.698	0.973	0.297	0.675	20
Meifu	0.724	0.963	0.014	0.948	25

Nat. Hazards Earth Syst. Sci. Discuss., doi:10.5194/nhess-2016-1, 2016
Manuscript under review for journal Nat. Hazards Earth Syst. Sci.
Published: 23 February 2016

Natural Hazards and Earth System Sciences Discussions

Table 4 Selection of associate site for the second model input based on $\overline{CC}$ and $\overline{MI}$

Candidate site	Target site											
	$\overline{CC}$ between cross-site water-levels				$\overline{MI}$ between water-level input from candidate site and cumulative rainfall input for target site				R (* highest)			
	Zongnan-xin	Xinnan	Sijie	Meifu	Zongnan-xin	Xinnan	Sijie	Meifu	Zongnan-xin	Xinnan	Sijie	Meifu
Zongnanxin	NA	0.815	0.763	0.703	NA	0.695	0.655	0.589	NA	1.120	1.108	1.114
Xinnan	0.815	NA	0.944	0.951	0.880	NA	0.721	0.657	0.935	NA	1.223*	1.295*
Sijie	0.763	0.944	NA	0.949	0.880	0.766	NA	0.657	0.883	1.178	NA	1.292
Meifu	0.703	0.951	0.949	NA	0.678	0.814	0.728	NA	1.024*	1.137*	1.221	NA
							Selected associate site		Meifu	Meifu	Xinnan	Xinnan

Table 5 Input variables for the water-level forecast models

Gauging site	Inputs			
	Cumulative rainfall (mm)		Water level (m)	
	Duration (hr)	Lag	Associate site	Lag
Zongnanxin	18	0	Meifu	0
Xinnan	20	0	Meifu	0
Sijie	20	0	Xinnan	0
Meifu	25	0	Xinnan	0

Nat. Hazards Earth Syst. Sci. Discuss., doi:10.5194/nhess-2016-1, 2016
Manuscript under review for journal Nat. Hazards Earth Syst. Sci.
Published: 23 February 2016

Natural Hazards and Earth System Sciences
Discussions

Table 6 Models selected from the Pareto optimal model set using the best scores for each of the three objectives (* best score)

Gauging site	Model	Objective	Design variables	$\overline{CE}$	$\overline{PE}$	$\overline{RTS}$
Zongnanxin	Z1	max $\overline{CE}$	[9 9 4 8]	0.815*	0.144	0.422
	Z2	min $\overline{PE}$	[1 4 1 1]	0.732	0.033*	0.844
	Z3	min $\overline{RTS}$	[10 10 8 6]	0.692	0.194	0.356*
Xinnan	X1	max $\overline{CE}$	[10 4 6 3]	0.820*	0.062	0.378
	X2	min $\overline{PE}$	[1 2 2 3]	0.667	0.025*	0.989
	X3	min $\overline{RTS}$	[5 5 4 3]	0.723	0.201	0.167*
Sijie	S1	max $\overline{CE}$	[8 3 2 1]	0.660*	0.117	0.678
	S2	min $\overline{PE}$	[1 1 1 2]	0.499	0.035*	0.989
	S3	min $\overline{RTS}$	[3 6 7 6]	0.103	0.256	0.333*
Meifu	M1	max $\overline{CE}$	[8 8 6 8]	0.653*	0.211	0.567
	M2	min $\overline{PE}$	[1 1 5 3]	0.546	0.018*	0.967
	M3	min $\overline{RTS}$	[9 5 7 5]	0.333	0.217	0.233*

Nat. Hazards Earth Syst. Sci. Discuss., doi:10.5194/nhess-2016-1, 2016
Manuscript under review for journal Nat. Hazards Earth Syst. Sci.
Published: 23 February 2016

Natural Hazards and Earth System Sciences
Discussions

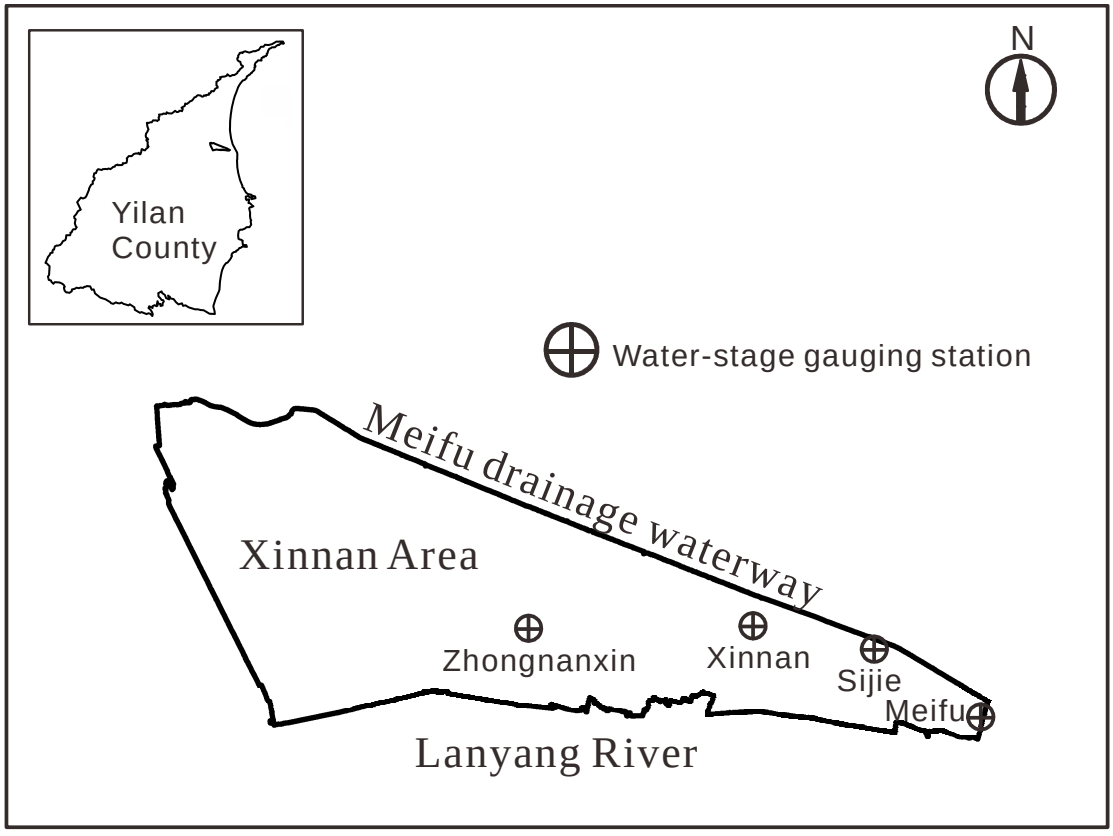

Figure 1 Xinnan area in Yilan County, Taiwan

Nat. Hazards Earth Syst. Sci. Discuss., doi:10.5194/nhess-2016-1, 2016
Manuscript under review for journal Nat. Hazards Earth Syst. Sci.
Published: 23 February 2016

Natural Hazards and Earth System Sciences
Discussions

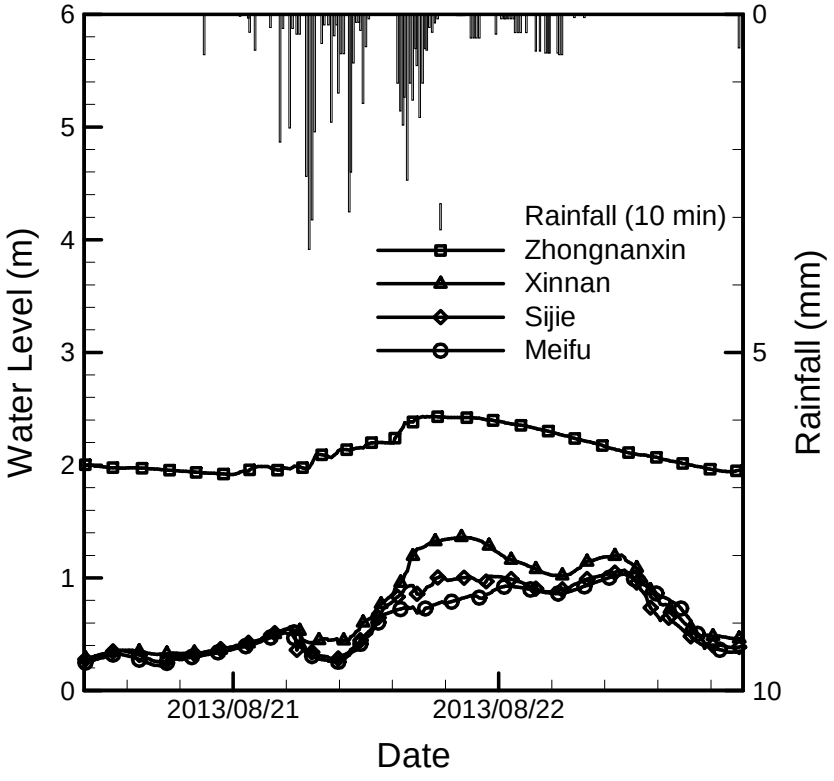

Figure 2 Rainfall and water-level data recorded by SNTIX during typhoon Trami

Nat. Hazards Earth Syst. Sci. Discuss., doi:10.5194/nhess-2016-1, 2016
Manuscript under review for journal Nat. Hazards Earth Syst. Sci.
Published: 23 February 2016

Natural Hazards and Earth System Sciences
Discussions

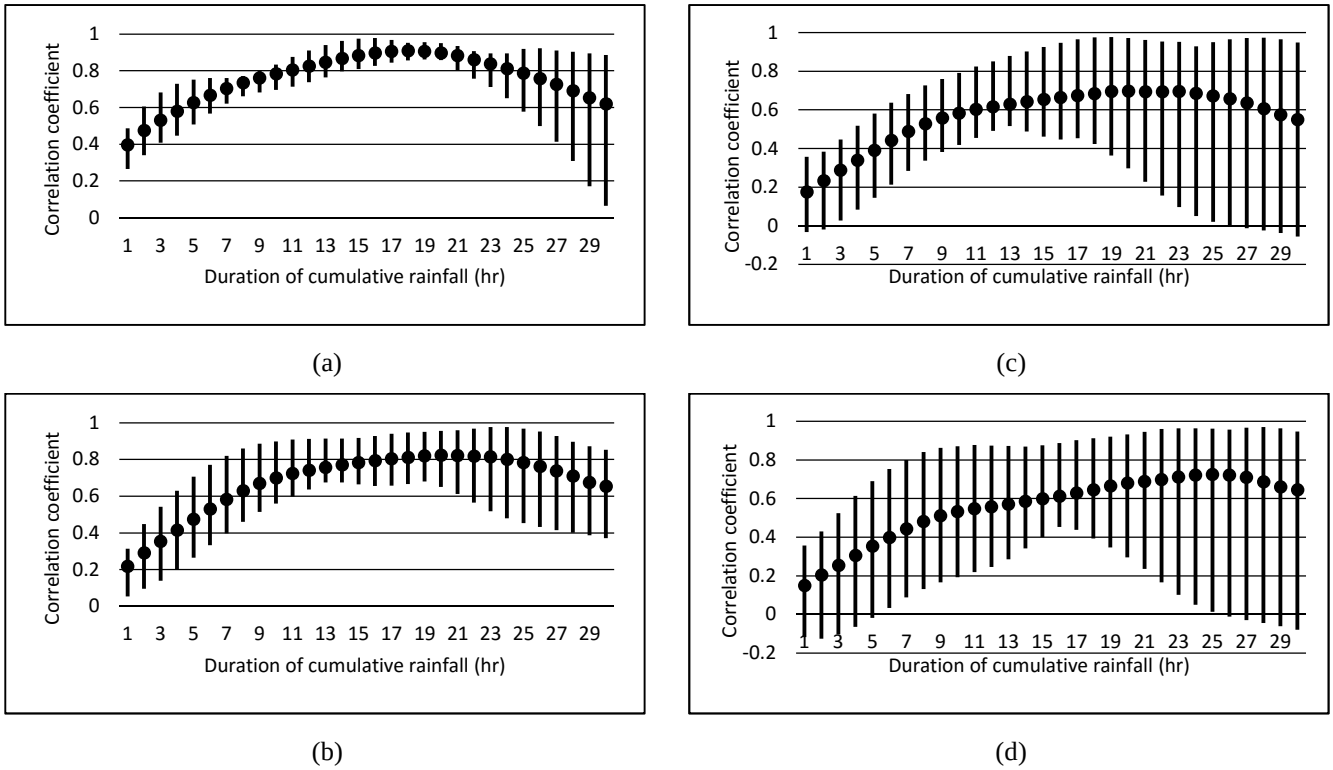

Figure 3 Correlations between water-level and cumulative rainfall over various durations (a) Zongnanxin station (b) Xinnan station (c) Sijie station (d) Meifu station

Nat. Hazards Earth Syst. Sci. Discuss., doi:10.5194/nhess-2016-1, 2016
Manuscript under review for journal Nat. Hazards Earth Syst. Sci.
Published: 23 February 2016

Natural Hazards and Earth System Sciences
Discussions

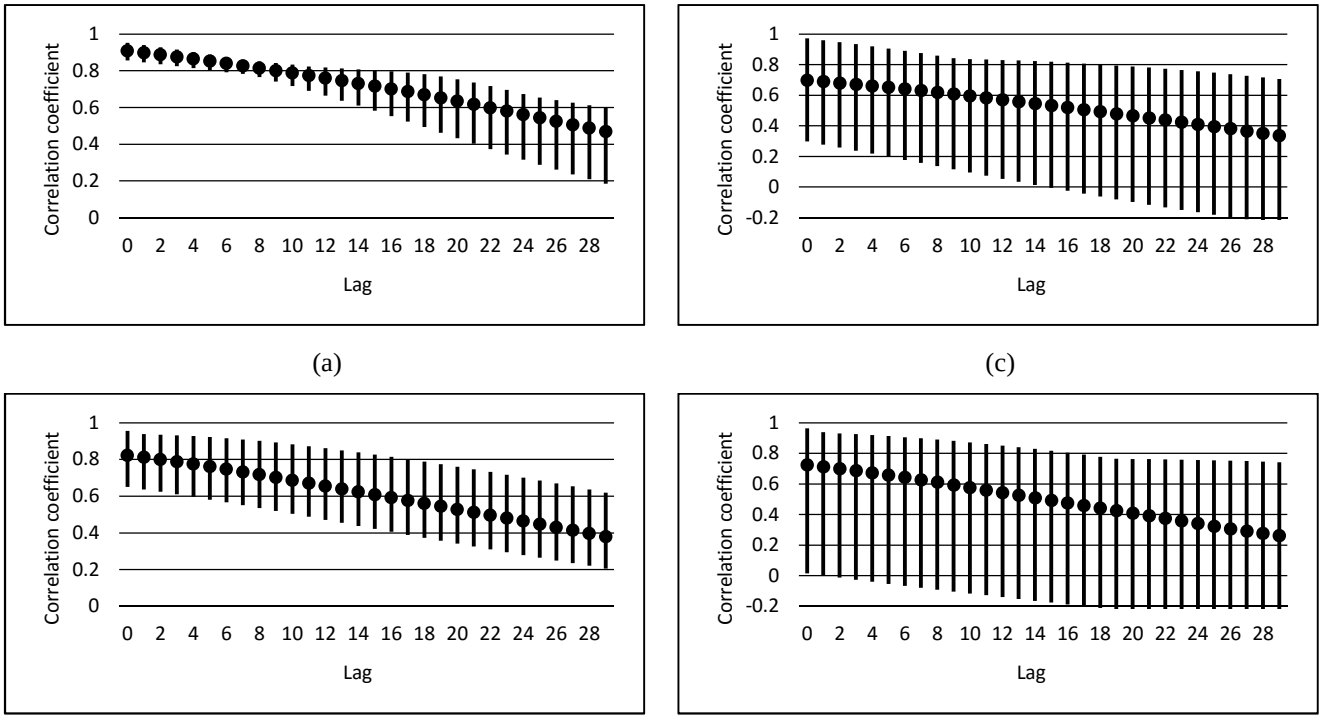

Figure 4 Cross-correlations between water-level and cumulative rainfall with various time lags (10 min per lag) (a) Zongnanxin station (b) Xinnan station (c) Sijie station (d) Meifu station (CC less than -0.2 is not shown)

Nat. Hazards Earth Syst. Sci. Discuss., doi:10.5194/nhess-2016-1, 2016
Manuscript under review for journal Nat. Hazards Earth Syst. Sci.
Published: 23 February 2016

Natural Hazards and Earth System Sciences
Discussions

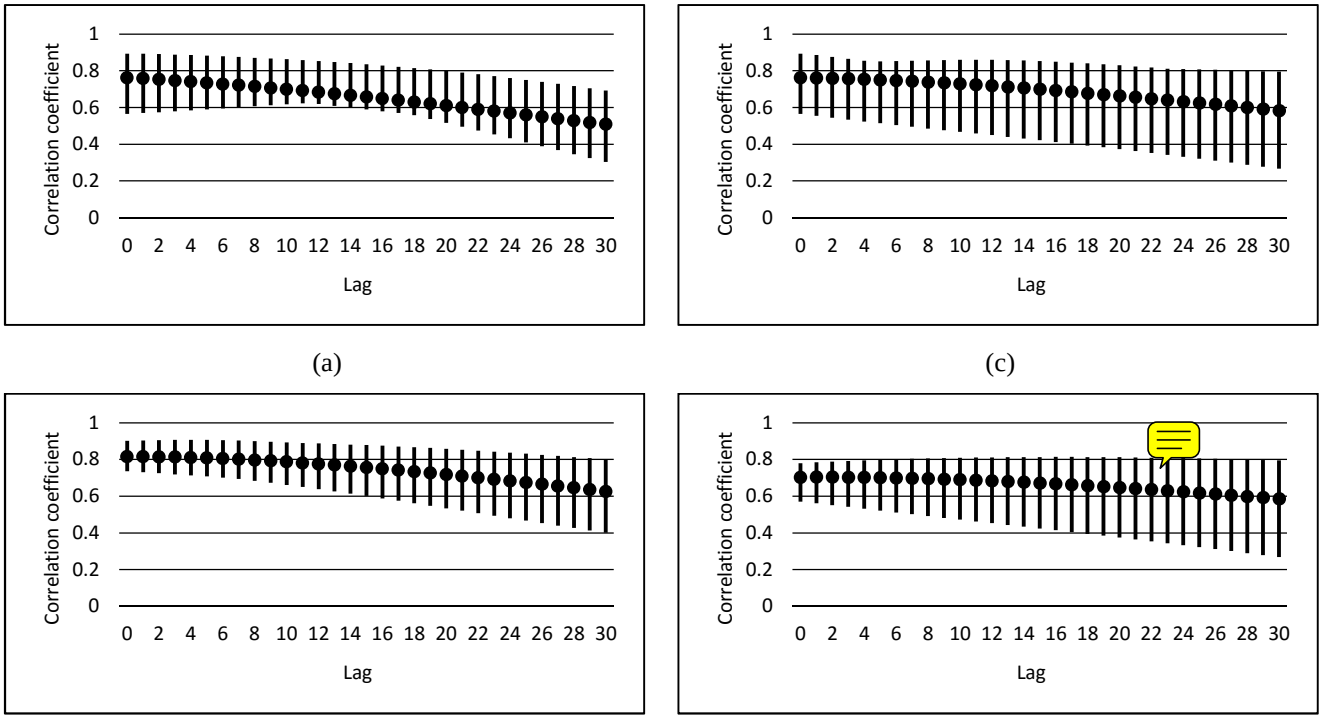

Figure 5 Cross-correlations of between-site water-levels with various time lags (10 min per lag) (a) Zongnanxin station (b) Xinnan station (c) Sijie station (d) Meifu station

Nat. Hazards Earth Syst. Sci. Discuss., doi:10.5194/nhess-2016-1, 2016
Manuscript under review for journal Nat. Hazards Earth Syst. Sci.
Published: 23 February 2016

Natural Hazards and Earth System Sciences
Discussions

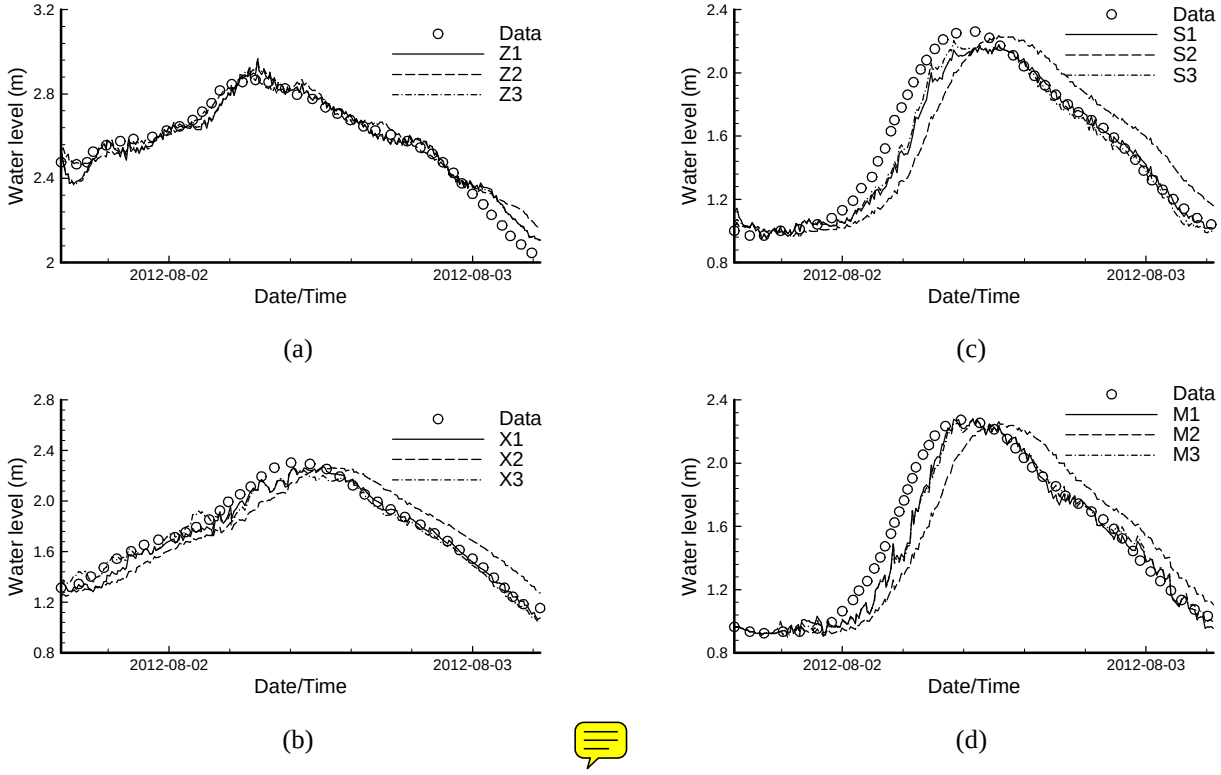

Figure 6 Comparison of model predictions (3-hr lead time) and measured data (a) Zongnanxin station (b) Xinnan station (c) Sijie station (d) Meifu station